Electron acoustic nonlinear structures in planetary magnetospheres

K. H. Shah, M. N. S. Qureshi, W. Masood, and H. A. Shah

Citation: Physics of Plasmas **25**, 042303 (2018); doi: 10.1063/1.5026186
View online: https://doi.org/10.1063/1.5026186
View Table of Contents: http://aip.scitation.org/toc/php/25/4
Published by the American Institute of Physics

Electron acoustic nonlinear structures in planetary magnetospheres

K. H. Shah,[1] M. N. S. Qureshi,[2,a)] W. Masood,[3,4] and H. A. Shah[1,2]
[1]*Department of Physics, FC College (A Chartered University), Lahore 54600, Pakistan*
[2]*Department of Physics, GC University, Lahore 54000, Pakistan*
[3]*COMSATS Institute of Information Technology, Islamabad 45550, Pakistan*
[4]*National Centre for Physics, QAU Campus, Islamabad 44000, Pakistan*

(Received 16 February 2018; accepted 22 March 2018; published online 6 April 2018)

In this paper, we have studied linear and nonlinear propagation of electron acoustic waves (EAWs) comprising cold and hot populations in which the ions form the neutralizing background. The hot electrons have been assumed to follow the generalized (r, q) distribution which has the advantage that it mimics most of the distribution functions observed in space plasmas. Interestingly, it has been found that unlike Maxwellian and kappa distributions, the electron acoustic waves admit not only rarefactive structures but also allow the formation of compressive solitary structures for generalized (r, q) distribution. It has been found that the flatness parameter r, tail parameter q, and the nonlinear propagation velocity u affect the propagation characteristics of nonlinear EAWs. Using the plasmas parameters, typically found in Saturn's magnetosphere and the Earth's auroral region, where two populations of electrons and electron acoustic solitary waves (EASWs) have been observed, we have given an estimate of the scale lengths over which these nonlinear waves are expected to form and how the size of these structures would vary with the change in the shape of the distribution function and with the change of the plasma parameters. *Published by AIP Publishing.*
https://doi.org/10.1063/1.5026186

I. INTRODUCTION

Electron acoustic waves (EAWs) are customarily high-frequency plasma waves where the inertia comes from a scant number of cold electrons while the restoring force comes from the dominant thermalized inertialess hot electrons and the ions form the neutralizing background. The validity of the fluid model requires the phase velocity of the electron acoustic wave to lie between the thermal velocities of cold and hot electrons. The electron acoustic wave has been observed to play an important role both in laboratory and space plasmas as the two populations of electrons have been frequently detected in these environments. EAWs have successfully been used to explain the electrostatic component of the broadband electrostatic noise (BEN) observed in the cusp of the terrestrial magnetosphere and in the geomagnetic tail.[1–4] Using Geotail spacecraft data, BEN has been shown to be composed of a single or a sequence of isolated electrostatic solitary waves (ESWs).[4] Observations from the Fast Auroral Snapshot (FAST) satellite[5] have shown the presence of single-period structures with large amplitudes (up to 2.5 V/m). These structures have been found to move faster than the ion acoustic speed and carry substantial potentials (up to 100 V). Two-electron temperature plasmas have also been observed in terrestrial bow shock, magnetosheath, magnetopause, the heliospheric termination shock, and planetary and neutron star magnetospheres. The linear[6–9] and nonlinear[7,10–12] properties of EAWs have extensively been studied in the literature. Very recently, in the Magnetized Plasma Linear Experimental device, the wave has been observed and seen to propagate with the phase velocity approximately 1.8 times the electron thermal velocity. A small amount of cold, drifting electrons, with the moderate bulk to cold temperature ratio (∼2–3) has also been found to be present in the device.

The electron distribution functions observed in space have been found to show a departure from the Maxwellian distribution. One of these distributions is kappa distribution which looks like Maxwellian at low energies but has modified tails at high energies. Kappa distributions with $2 \leq \kappa \leq 6$ have been found to fit the observations and satellite data in the solar wind,[13] the terrestrial magnetosphere,[14] the terrestrial plasmasheet,[15–17] the magnetosheath,[18] the radiation belts,[19] the magnetosphere of other planets such as Mercury,[20] the magnetosphere of Jupiter,[21] the Io plasma torus as observed by Ulysses[22] and Cassini,[23] and so on and so forth. In the auroral region, Freja and Viking satellites observed the density depletion structures which were explained by another non-Maxwellian Cairns distribution. However, electron distributions have been observed in regions of space plasmas with modified tails and flat tops. Such distributions differ significantly from kappa and Cairns distribution functions. More than a decade ago, Qureshi *et al.*[24] constructed a new non-Maxwellian distribution function comprising two spectral indices r and q, instead of one spectral index used in the kappa distribution function to explain the observed phenomena in space plasmas in a more thorough manner. It would be beneficial to mention here that (r, q) distribution has an immense advantage over the other distribution functions as it can impersonate almost all the distribution functions by using different choices of r and q.[18]

The paper is arranged as follows: In Sec. II, we first introduce the generalized (r, q) distribution and explain how the two spectral indices r and q modify the shape of the distribution

a)Author to whom correspondence should be addressed: nouman_sarwar@yahoo.com and nouman_sarwar25@hotmail.com

function. We then present the basic set of equations governing the system under consideration. In Sec. III, we lay down the stretching and perturbation scheme to derive the nonlinear Korteweg de Vries (KdV) equation for the ion acoustic waves in which the electrons follow the generalized (r,q) distribution. We also explore in detail the effect of spectral indices r and q on the propagation characteristics of linear and nonlinear electron acoustic waves. Finally, main findings of this paper have been recapitulated in Sec. IV.

II. MODEL DISTRIBUTION AND EQUATIONS

Distribution functions observed in the Earth's magnetosphere such as in the magnetosheath[25–27] and polar cusp[28] often show distinct features which are not present in the Maxwellian and kappa distributions. These observed distributions have flat top or shoulders at low energies superimposed by either Maxwellian or superthermal tails.[17,24] The presence of flat top or shoulders cannot be modeled by either Maxwellian or kappa distribution and the only way to represent them is generalized (r,q) distribution function which has the following functional form:

$$F_{rq}(v)=\frac{\alpha}{\pi\,(v_t)^{3/2}}\left(1+\frac{1}{q-1}\left\{\frac{v^2-2e\phi/m_e}{\beta\,(2T_e/m_e)}\right\}^{r+1}\right)^{-q}, \tag{1}$$

where

$$\alpha=\frac{3\,\Gamma[q]\,(q-1)^{-3/(2+2r)}}{4\,\beta^{3/2}\,\Gamma\left[q-\frac{3}{2+2r}\right]\Gamma\left[1+\frac{3}{2+2r}\right]}, \tag{2}$$

$$\beta=\frac{3\,(q-1)^{-1/(1+r)}\,\Gamma\left[q-\frac{3}{2+2r}\right]\Gamma\left[\frac{3}{2+2r}\right]}{2\,\Gamma\left[q-\frac{5}{2+2r}\right]\Gamma\left[\frac{5}{2+2r}\right]}. \tag{3}$$

Here, r and q are the two spectral indices representing the degree of flatness and suprathermal particles in the distribution function, respectively, and satisfy the conditions $q>1$ and $q(r+1)>5/2$. Also, ϕ, Γ, $v_t=\sqrt{\frac{2T_e}{m_e}}$, T_e are the electrostatic potential, gamma function, thermal velocity, and electron temperature, respectively.

We can obtain the hot electron number density by integrating the distribution function (1) over the velocity space which is given here as under

$$n_h=n_{h0}\left(1+A\,\phi+B\,\phi^2\right). \tag{4}$$

Here, $\phi=e\phi/T_h$, and

$$A=\frac{(q-1)^{-1/(1+r)}\,\Gamma\left[q-\frac{1}{2+2r}\right]\Gamma\left[\frac{1}{2+2r}\right]}{2\,\beta\,\Gamma\left[q-\frac{3}{2+2r}\right]\Gamma\left[\frac{3}{2+2r}\right]}, \tag{5}$$

$$B=-\frac{(1+4\,r)(q-1)^{-2/(1+r)}\Gamma\left[q+\frac{1}{2+2r}\right]\Gamma\left[\frac{-1}{2+2r}\right]}{8\,\beta^2\,\Gamma\left[q-\frac{3}{2+2r}\right]\Gamma\left[\frac{3}{2+2r}\right]}. \tag{6}$$

The above constants A and B in Eqs. (5) and (6) reduce to constants for kappa distribution, i.e., $A=\frac{\kappa-1/2}{\kappa-3/2}$ and $B=\frac{(\kappa-1/2)(\kappa+1/2)}{2\,(\kappa-3/2)^2}$ in the limit $r=0$, $q\to(\kappa+1)$ and for Maxwellian distribution, i.e., $A=1$ and $B=1/2$ in the limit $r=0$, $q\to\infty$.[21,29]

Before we go on and describe the nonlinear evolution for electron acoustic waves, it is imperative that we write down a few lines about the existence of two-electron temperature plasma which is a pre-requisite for the propagation of electron acoustic waves (EAWs). The genesis of the multi-species model for identical particles dates to the days when it was used as an initial condition in the theoretical study of electron beam systems.[30] It was shown by Ikezawa and Nakamura[31] that the addition of a hot component in addition to the cold one will exacerbate the Landau damping of the electron acoustic wave and they also gave an estimate of the electron-electron collisions and interestingly noted that the relaxation time is shorter than the collision time which suggested another mechanism besides collisions for the relaxation of two-electron species. Yu and Luo[32] wrote a brilliant article about the limitations of multi-species models used for the same mass species. It was suggested that the multi-species model makes more sense when the two electrons are physically separated in phase space and there is no chance of the mixing explained above. He presented a couple of scenarios including trapping of particles that could help us construct a reasonable multi-species model for identical species. In our model, we have taken the dynamics of cold electrons and hot species have been assumed to be governed by the generalized (r,q) distribution. Such a scenario is possible in space plasmas as the particles can come from a different region of space where the physical conditions were different. The magnetosphere is replete with such observations. The additional advantage of assuming such a situation is that electron-electron collisions no longer pose the technical difficulty as the two electron-populations do not belong to the same phase space distribution function. The above-mentioned examples of the observations of electron acoustic waves in space plasmas fortify our assumption.

To study the propagation of nonlinear electron acoustic solitary waves (EASWs), we consider collisionless, homogeneous, and unmagnetized plasma comprising cold electrons, (r,q) distributed hot electrons, and immobile ions. The model equations in one dimension are governed by the following set of continuity, momentum, and Poisson's equations:

$$\frac{\partial n_c}{\partial t}+\frac{\partial\,(n_c v_c)}{\partial x}=0, \tag{7}$$

$$\frac{\partial v_c}{\partial t}+v_c\frac{\partial v_c}{\partial x}=\gamma\frac{\partial\phi}{\partial x}, \tag{8}$$

$$\frac{\partial^2\phi}{\partial x^2} = \frac{1}{\gamma} n_c + n_h - \left(1 + \frac{1}{\gamma}\right). \tag{9}$$

Here, n_h and n_c are hot and cold electron number densities normalized by background number density n_0, $\gamma = \frac{n_{h0}}{n_{c0}}$ is the ratio of hot to cold electrons, and v_c is cold electron velocity normalized by $c_e = \left(\frac{T_h}{\gamma m}\right)^{\frac{1}{2}}$, whereas time and space are normalized by $\omega_{pi}^{-1} = \sqrt{\frac{\epsilon_0 m}{n_{c0} e^2}}$ and $\lambda_{Dh} = \sqrt{\frac{\varepsilon_0 T_h}{n_{h0} e^2}}$, respectively.

To derive the nonlinear Korteweg de Vries (KdV) equation for EAWs, the following stretched coordinates are used:

$$\xi = \varepsilon^{\frac{1}{2}}(x - V_0 t) \quad \text{and} \quad \tau = \varepsilon^{3/2} t, \tag{10}$$

where ε is a small parameter representing the strength of nonlinearity and V_0 is the phase velocity of the solitary wave. Using the reductive perturbation method,[17] n, v, and ϕ in perturbed form can be written as

$$n_c = 1 + \varepsilon\, n_{1c} + \varepsilon^2 n_{2c} + \cdots, \tag{11}$$

$$v_c = \varepsilon\, v_{1c} + \varepsilon^2 v_{2c} + \cdots, \tag{12}$$

$$\varphi = \varepsilon\, \phi_1 + \varepsilon^2 \phi_2 + \cdots. \tag{13}$$

Equations (7)–(9) in lowest order in ε are given below,

$$V_0 n_{1c} = v_{1c}, \tag{14}$$

$$V_0 v_{1c} = -\gamma \phi_1, \tag{15}$$

$$V_0 = \frac{1}{\sqrt{A}}. \tag{16}$$

For the next higher order in ε, Eqs. (7)–(9) yield

$$\frac{\partial n_{1c}}{\partial \tau} - V_0 \frac{\partial n_{2c}}{\partial \xi} + \frac{\partial v_{2c}}{\partial \xi} + \frac{\partial (n_{1c} v_{1c})}{\partial \xi} = 0, \tag{17}$$

$$\frac{\partial v_{1c}}{\partial \tau} - V_0 \frac{\partial v_{2c}}{\partial \xi} + v_{1c} \frac{\partial v_{1c}}{\partial \xi} - \gamma \frac{\partial \phi_2}{\partial \xi} = 0, \tag{18}$$

$$\frac{\partial^2 \phi_1}{\partial x^2} = \frac{1}{\gamma} n_{2c} + A\, \phi_2 + B\, {\phi_1}^2. \tag{19}$$

The algebraic manipulation of Eqs. (17)–(19) leads to the following KdV equation for the EAWs with generalized (r,q) distribution:

$$\frac{\partial \phi_1}{\partial \tau} + C \frac{\partial \phi_1^2}{\partial \xi} + D \frac{\partial^3 \phi_1}{\partial \xi^3} = 0, \tag{20}$$

where

$$C = -\frac{1}{2}\left(\frac{3\gamma}{2V_0} + {V_0}^3 B\right) \quad \text{and} \quad D = \frac{{V_0}^3}{2}. \tag{21}$$

For the sake of completeness, it suffices to say that C is the coefficient of nonlinearity, whereas D is the dispersive coefficient. The solution of KdV equation (20) can be written as

$$\phi = \frac{3u}{C} \mathrm{Sech}\left[\frac{\xi}{\Delta}\right]^2, \tag{22}$$

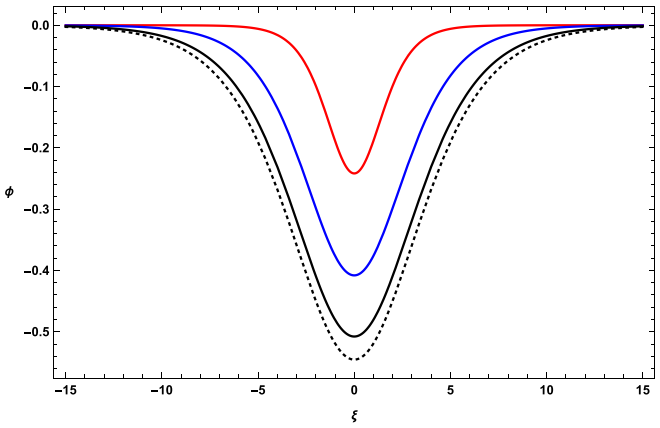

FIG. 1. KdV electron-acoustic rarefactive solitary structures for (r, q) distribution in the limiting cases for Maxwellian distribution when $r = 0$ and $q \to \infty$ (dotted), and kappa distribution when $r = 0$ and $q = 3$ (red), 5 (blue), and 15 (black). The other parameters are $\gamma = 0.4$ and $u = 0.1$.

where u is the velocity of the nonlinear structure and $\Delta = \sqrt{\frac{4D}{u}}$ is the width of the solitary structure.

III. NUMERICAL RESULTS

Figure 1 depicts the rarefactive solitary structures obtained in the limiting cases when $r = 0$, $q \to \infty$ (Maxwellian) and $r = 0$, $q \to \kappa + 1$ (kappa) of KdV equation given by Eq. (20). In both cases, we find rarefactive solitary structures and if spectral index q increases, solitary structures approach towards the Maxwellian case.

Figure 2 manifests the behavior of electron acoustic rarefactive solitary structures for different values of the flatness parameter r when q is kept fixed. It is found that the increasing value of r mitigates the amplitude of the solitary structure; however, the width of the solitary structure enhances. Figure 3 explores the behavior of nonlinear EAWs for different negative values of r, which represent a spiky distribution function, by keeping q constant. We note that an increase in the negative value of r brings about an increase in the amplitude of the solitary structures. If we further increase the negative value of r, the polarity of the solitary structures reverses and we obtain compressive solitary structures. This

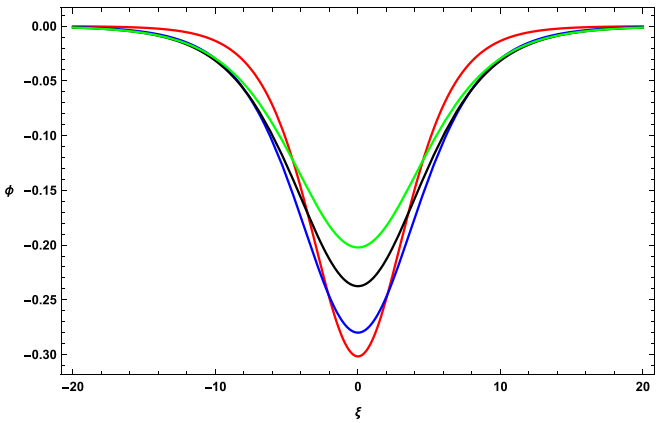

FIG. 2. KdV electron-acoustic rarefactive solitary structures for different values of $r = 1$ (red), 2 (blue), 3 (black), and 4 (green) when $q = 2$, $\gamma = 0.4$, and $u = 0.1$.

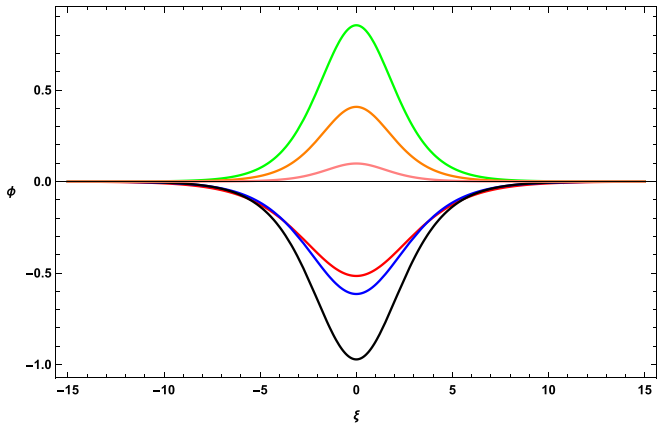

FIG. 3. KdV electron-acoustic rarefactive solitary structures for different negative values of $r = -0.1$ (red), -0.2 (blue) -0.27 (black) and compressive solitary structures soliton $r = -0.35$ (green), -0.37 (orange) and -0.35 (pink) when $q = 10$, $\gamma = 0.4$, and $u = 0.1$.

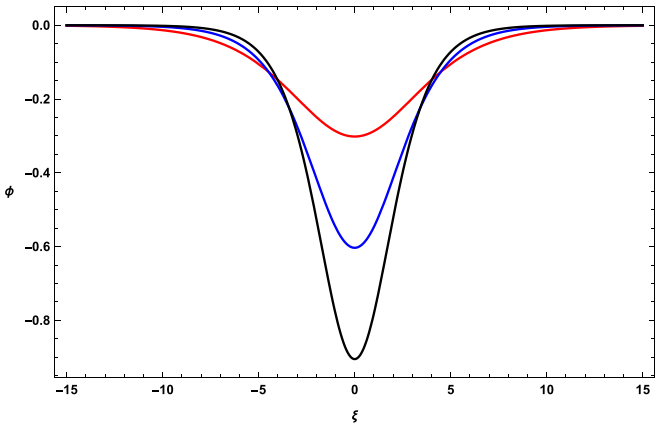

FIG. 5. KdV electron-acoustic rarefactive solitary structures for different values of $u = 0.1$ (red), 0.2 (blue), and 0.3 (black) when $\gamma = 0.4$, $q = 2$, and $r = 1$.

is indeed quite interesting and reflects the complex interplay between the terms appearing in the nonlinearity coefficient of the KdV equation. It is pertinent to mention here that the sign of the nonlinearity coefficients determines the polarity of the nonlinear electron acoustic solitary structures.

Figure 4 shows the behavior of electron acoustic rarefactive solitary structures for different values of q for the fixed value of r. We can see that if the value of q increases the amplitude of the solitary structures also increases in terms of magnitude. Figure 5 shows the behavior of rarefactive solitary structures for different values of propagation velocity u when the values of r and q are kept fixed. We can see that as the value of u increases the amplitude of the rarefactive soliton increases. Figures 6–8 show the maximum amplitude of solitary structures against the possible ranges of propagation velocity u for different values of r and q. Figure 6 depicts the maximum amplitude of the rarefactive solitary structures versus the possible range of the propagation velocity u for different values of positive r when $\gamma = 0.4$ and $q = 2$ (thin line), $q = 10$ (thick line). We can see that rarefactive solitary structures could be obtained for large values of u when $r = 3$ and this range decreases as r becomes smaller. For a fixed value of r, the range of propagation velocity decreases as q becomes smaller.

Figure 7 manifests the maximum amplitude of the rarefactive solitary structures versus the possible range of the propagation velocity u for different values of negative r when $\gamma = 0.4$ and $q = 5$ (thin line), and $q = 10$ (thick line). We can see that rarefactive solitary structures could be obtained for large values of u when $r = -0.1$ and this range decreases as the negative value of r increases. For a fixed value of r, the range of propagation velocity increases when q increases. Finally, Fig. 8 shows the maximum amplitude of the compressive solitary structures against the possible range of the propagation velocity u for different values of negative r when $\gamma = 0.4$ and $q = 5$ (thin line), and $q = 10$ (thick line). We can see that rarefactive solitary structures could be obtained for large values of u when the negative value of r increases. For a fixed value of r, the range of propagation velocity increases with the increase in values of q.

Since two components of electrons are frequently observed in space plasmas, we can estimate the scale lengths of the structures from these regions based on the observed parameters. Observations from Saturn's magnetosphere

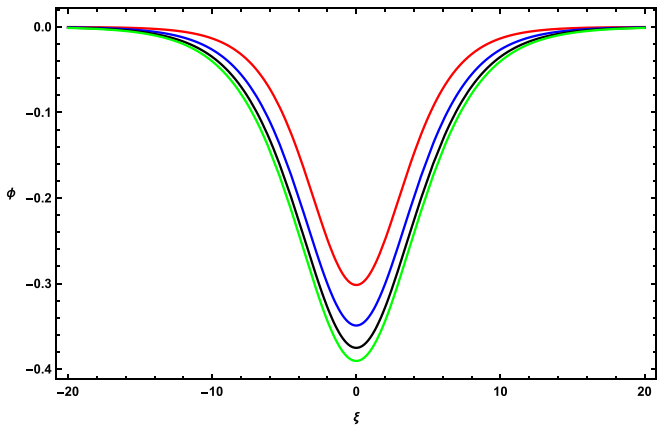

FIG. 4. KdV electron-acoustic rarefactive solitary structures for different negative values of $q = 2$ (red), 3 (blue), 5 (black), and 10 (green) when $r = 1$, $\gamma = 0.4$, and $u = 0.1$.

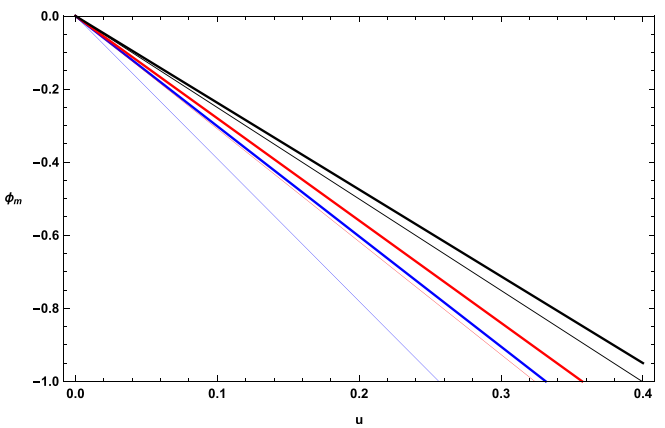

FIG. 6. Maximum amplitude of electron-acoustic rarefactive solitary structures against the propagation velocity u for different values of $r = 1$ (blue), 2 (red), 3 (black) when $\gamma = 0.4$, $q = 2$ (thin line), and 10 (thick line).

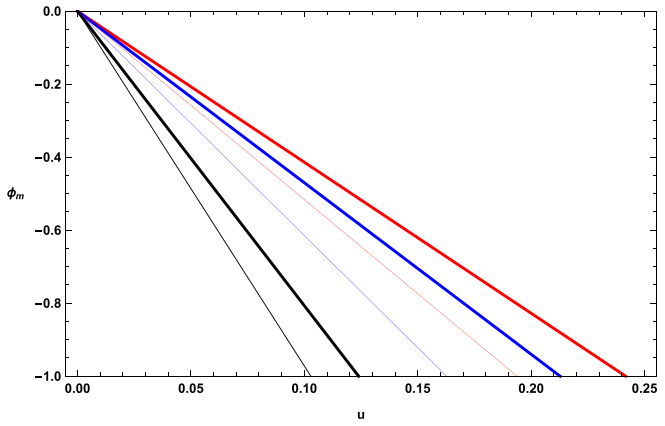

FIG. 7. Maximum amplitude of electron-acoustic rarefactive solitary structures against the propagation velocity u for different negative values of $r = -0.1$ (red), -0.2 (blue), -0.3 (black) when $\gamma = 0.4$, $q = 5$ (thin line), and 10 (thick line).

show that hot electrons have temperatures in the range 400–1000 eV and densities vary from 0.01–0.18 cm^{-3}.[33] From the solitary structures plotted in Figs. 1–5, the scale length of the rarefactive solitary structures for Maxwellian and kappa distribution lies in the range of 15–45 km and 5–30 km, respectively, whereas the scale length of the rarefactive solitary structures for the case of (r, q) distribution lies in the range of 10–60 km for positive values of r and 10–30 km for negative values of r. The scale length of compressive solitary structures, which are only observed for (r, q) distribution, lies in the range 5–30 km. In the Earth's auroral region, hot electrons are observed with densities 1.5–2.0 cm^{-3} and temperature 250 eV.[34] Corresponding to Figs. 1–5, the scale length of the rarefactive solitary structures for Maxwellian and kappa distribution lies in the range of 2.5–2.9 km and 0.8–1.92 km, respectively. The scale length of the rarefactive solitary structures for the case of (r, q) distribution lies in the range of 1.66–3.84 km for positive values of r and 1.66–1.92 km for negative values of r where compressive solitary structures have scale lengths in the range 0.8–1.92 km.

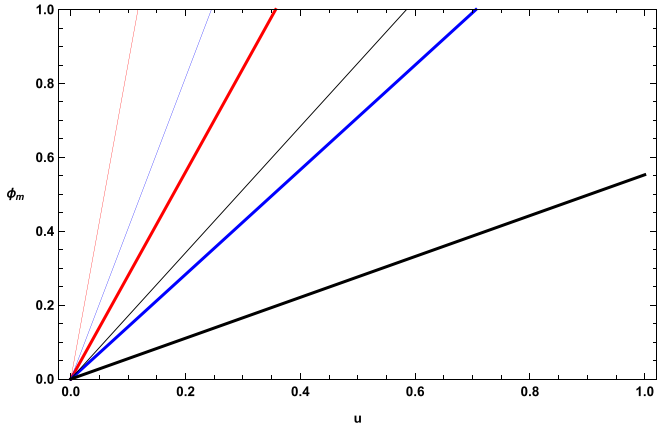

FIG. 8. Maximum amplitude of electron-acoustic compressive solitary structures against the propagation velocity u for different negative values of $r = -0.35$ (red), -0.37 (blue), -0.4 (black) when $\gamma = 0.4$, $q = 5$ (thin line), and 10 (thick line).

IV. CONCLUSION

In this paper, we have studied the nonlinear propagation of electron acoustic waves in the presence of electrons which follow the generalized (r, q) distribution. It is fairly well known that only rarefactive solitary structures can be obtained when electrons obey Maxwellian or kappa distributions. However, interestingly, it has been found that when electrons follow a generalized (r, q) distribution function, the nonlinear electron acoustic waves admit both rarefactive and compressive solitary structures. For positive values of r that correspond to a flat-topped distribution, we have found density depletions or rarefactive solitary structures which had been detected by Freja and Viking satellites.[13,35] It has been shown that the flatness parameter r, tail parameter q, and the propagation velocity of the nonlinear structure significantly modify the propagation characteristics of nonlinear electron acoustic solitary waves. Using the plasma parameters typically found in Saturn's magnetosphere and Earth's auroral region, we have presented an estimate of the spatial scales over which the nonlinear EAWs are expected to form. A very recent study reports the existence of electron acoustic solitary structures that have spatial scales of the order of a kilometer in the inner magnetosphere[36] which support our estimates based on theoretical modelling of these structures.

ACKNOWLEDGMENTS

This research was supported by the Higher Education Commission (HEC) Grant No. 20-2595/NRPU/R&D/HEC/13.

[1]R. L. Tokar and S. P. Gary, Geophys. Res. Lett. **11**, 1180, https://doi.org/10.1029/GL011i012p01180 (1984).
[2]R. Pottelette, M. Malingre, N. Dubouloz, B. Aparicio, and R. Lundin, J. Geophys. Res. **95**, 5957, https://doi.org/10.1029/JA095iA05p05957 (1990).
[3]N. Dubouloz, R. Pottelette, M. Malingre, G. Holmgren, and P. A. Lindqvist, J. Geophys. Res. **96**, 3565, https://doi.org/10.1029/90JA02355 (1991).
[4]H. Matsumoto, H. Kojima, T. Miyatake, Y. Omura, M. Okada, I. Nagano, and M. Tsutsui, Geophys. Res. Lett. **21**, 2915, https://doi.org/10.1029/94GL01284 (1994); D. Schriver and M. Ashour-Abdalla, *ibid.* **16**, 899, https://doi.org/10.1029/GL016i008p00899 (1989).
[5]R. E. Ergun, C. W. Carlson, J. P. McFadden, F. S. Mozer, G. T. Delory, W. Peria, C. C. Chaston, M. Temerin, I. Roth, L. Muschietti, R. Eliphic, R. Strangeway, R. Pfaff, C. A. Cattell, D. Klumpar, E. Shelley, W. Peterson, E. Moeblus, and L. Kistler, Geophys. Res. Lett. **25**, 2041, https://doi.org/10.1029/98GL00636 (1998).
[6]R. L. Mace and M. A. Hellberg, J. Plasma Phys. **43**, 239 (1990).
[7]M. P. Dell, I. M. A. Geldhill, and M. A. Hellberg, Z. Naturforsch. A: Phys. Sci. **42**, 1175 (1987).
[8]M. Yu and P. K. Shukla, J. Plasma Phys. **29**, 409 (1983).
[9]S. P. Gary and R. L. Tokar, Phys. Fluids **28**, 2439 (1985).
[10]M. Berthomier, R. Pottelette, M. Malingre, and Y. Khotyainsev, Phys. Plasmas **7**, 2987 (2000); W. Masood and H. A. Shah, J. Fusion Energy **22**, 201 (2003).
[11]N. Dubouloz, R. Pottelette, M. Malingre, and R. A. Treumann, Geophys. Res. Lett. **18**, 155, https://doi.org/10.1029/90GL02677 (1991).
[12]R. L. Mace, S. Baboolal, R. Bharuthram, and M. A. Hellberg, J. Plasma Phys. **45**, 323 (1991).
[13]R. Bostrom, IEEE Trans. Plasma Sci. **20**, 756 (1992).
[14]A. I. Eriksson, B. Holback, P. O. Dovner, R. Boström, G. Holmgren, M. Andrd, L. Eliasson, and P. M. Kinruer, Geophys. Res. Lett. **21**, 1843, https://doi.org/10.1029/94GL00174 (1994).
[15]J. L. Vago, P. M. Kintner, S. W. Chesney, R. L. Arnoldy, K. A. Lynch, T. E. Moore, and C. J. Pollock, J. Geophys. Res. **97**, 16935, https://doi.org/10.1029/92JA01526 (1992).

[16]R. A. Cairns, A. A. Mamun, R. Bingham, R. Boström, R. O. Dendy, C. M. C. Nairn, and P. K. Shukla, Geophys. Res. Lett. **22**, 2709, https://doi.org/10.1029/95GL02781 (1995).
[17]M. N. S. Qureshi, J. K. Shi, and S. Z. Ma, Phys. Plasmas **12**, 122902 (2005).
[18]M. N. S. Qureshi, W. Nasir, W. Masood, P. H. Yoon, H. A. Shah, and S. J. Schwartz, J. Geophys. Res. **119**, 10059, https://doi.org/10.1002/2014JA020476 (2014).
[19]Z. Kiran, H. A. Shah, M. N. S. Qureshi, and G. Murtaza, Sol. Phys. **236**, 167 (2006).
[20]T. K. Balaku and M. A. Hellberg, Phys. Plasmas **15**, 123705 (2008).
[21]W. Masood, M. N. S. Qureshi, P. H. Yoon, and H. A. Shah, J. Geophys. Res. **120**, 101, https://doi.org/10.1002/2014JA020459 (2015).
[22]H. Washimi and T. Tanuiti, Phys. Rev. Lett. **17**, 996 (1966).
[23]D. Zhao, S. Fu, G. K. Parks, W. Sun, Q. Zong, D. Pan, and T. Wu, Phys. Plasmas **24**, 082903 (2017).
[24]M. N. S. Qureshi, H. A. Shah, G. Murtaza, S. J. Schwartz, and F. Mahmood, Phys. Plasmas **11**, 3819–3829 (2004).
[25]M. D. Montgomery, J. R. Asbridge, and S. J. Bame, J. Geophys. Res. **75**, 1217, https://doi.org/10.1029/JA075i007p01217 (1970).
[26]W. C. Feldman, R. C. Anderson, S. J. Bame, J. T. Gosling, and R. D. Zwickl, J. Geophys. Res. **88**, 9949, https://doi.org/10.1029/JA088iA12p09949 (1983).
[27]W. Masood, S. J. Schwartz, M. Maksimovic, and A. N. Fazakerley, Ann. Geophys. **24**, 1725–1735 (2006).
[28]G. K. Parks, E. Lee, N. Lin, F. Mozer, M. Wilber, I. Dandouras, H. Reme, E. Lucek, A. Fazakerley, M. Goldstein, C. Gurgiolo, P. Canu, N. Cornilleau-Wehrlin, and P. Decreau, Phys. Rev. Lett. **98**, 265001 (2007).
[29]C. R. Choi, K. W. Min, and T. N. Rhee, Phys. Plasmas **18**, 092901 (2011).
[30]A. Hasegawa, Rev. Geophys. Space Phys. **9**, 703, https://doi.org/10.1029/RG009i003p00703 (1971).
[31]S. Ikezawa and Y. Nakamura, J. Phys. Soc. Jpn. **50**, 962 (1981).
[32]M. Y. Yu and H. Luo, Phys. Plasmas **15**, 024504 (2008).
[33]P. Schippers, M. Blanc, N. Andre, I. Dandouras, G. R. Lewis, L. K. Gilbert, A. M. Persoon, N. Krupp, D. A. Gurnett, A. J. Coates, S. M. Krimigis, D. T. Young, and M. K. Dougherty, J. Geophys. Res. **113**, A07208, https://doi.org/10.1029/2008JA013098 (2008).
[34]N. Dubouloz, R. A. Treumann, R. Pottelette, and M. Malingre, J. Geophys. Res. **98**, 17415, https://doi.org/10.1029/93JA01611 (1993).
[35]P. O. Dovner, A. I. Eriksson, R. Bostrom, and B. Holback, Geophys. Res. Lett. **21**, 1827, https://doi.org/10.1029/94GL00886 (1994).
[36]C. S. Dillard, I. Y. Vasko, F. S. Mozer, O. V. Agapitov, and J. W. Bonnell, Phys. Plasmas **25**, 022905 (2018).